

GENERALIZABLE LIGHTWEIGHT PROXY FOR ROBUST NAS AGAINST DIVERSE PERTURBATIONS

Hyeonjeong Ha^{1*}, Minseon Kim^{1*}, Sung Ju Hwang^{1,2}

¹Korea Advanced Institute of Science and Technology (KAIST), ²AITRICS
{hyeonjeongha, minseonkim, sjhwang82}@kaist.ac.kr

ABSTRACT

Recent neural architecture search (NAS) frameworks have been successful in finding optimal architectures for given conditions (e.g., performance or latency). However, they search for optimal architectures in terms of their performance on clean images only, while robustness against various types of perturbations or corruptions is crucial in practice. Although there exist several robust NAS frameworks that tackle this issue by integrating adversarial training into one-shot NAS, however, they are limited in that they only consider robustness against adversarial attacks and require significant computational resources to discover optimal architectures for a single task, which makes them impractical in real-world scenarios. To address these challenges, we propose a novel lightweight robust zero-cost proxy that considers the consistency across features, parameters, and gradients of both clean and perturbed images at the initialization state. Our approach facilitates an efficient and rapid search for neural architectures capable of learning generalizable features that exhibit robustness across diverse perturbations. The experimental results demonstrate that our proxy can rapidly and efficiently search for neural architectures that are consistently robust against various perturbations on multiple benchmark datasets and diverse search spaces, largely outperforming existing clean zero-shot NAS and robust NAS with reduced search cost.

1 INTRODUCTION

Neural architecture search (NAS) techniques have achieved remarkable success in optimizing neural networks for given tasks and constraints, yielding networks that outperform handcrafted neural architectures (Baker et al., 2017; Liu et al., 2018a; Luo et al., 2018; Pham et al., 2018; Xu et al., 2020). However, previous NAS approaches have primarily aimed to search for architectures with optimal performance and efficiency on clean inputs, while paying less attention to robustness against adversarial perturbations (Goodfellow et al., 2015; Madry et al., 2018) or common types of corruptions (Hendrycks and Dietterich, 2019). This can result in finding unsafe and vulnerable architectures with erroneous and high-confidence predictions on input examples even with small perturbations (Mok et al., 2021; Jung et al., 2023), limiting the practical deployment of NAS in real-world safety-critical applications.

To address the gap between robustness and NAS, previous robust NAS works (Mok et al., 2021; Guo et al., 2020) have proposed to search for adversarially robust architectures by integrating adversarial training into NAS. Yet, they are computationally inefficient as they utilize costly adversarial training on top of the one-shot NAS methods (Liu et al., 2019; Cai et al., 2019), requiring up to $33\times$ larger computational cost than clean one-shot NAS (Xu et al., 2020). Especially, Guo et al. (2020) takes almost 4 GPU days on NVIDIA 3090 RTX GPU to train the supernet, as it requires performing adversarial training on subnets with perturbed examples (Figure 2, RobNet). Furthermore, they only target a single type of perturbation, i.e., adversarial perturbation (Goodfellow et al., 2015; Madry et al., 2018), thus, failing to generalize to diverse perturbations. In order to deploy NAS to real-world applications that require handling diverse types of tasks and perturbations, we need a lightweight NAS method that can yield robust architectures without going over such costly processes.

*Equal contribution. Author ordering determined by coin flip.

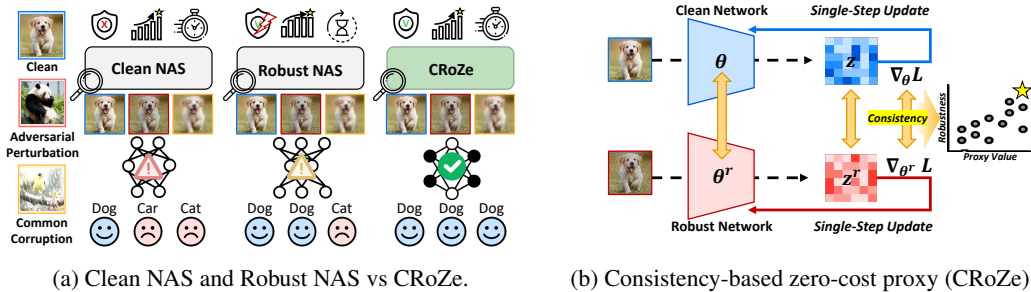


Figure 1: **Generalizable lightweight proxy for robust NAS against diverse perturbations.** While previous NAS methods search for neural architectures primarily on clean samples (Clean NAS) or adversarial perturbations (Robust NAS) with excessive search costs and fail to generalize across diverse perturbations, our proposed proxy, namely CRoZe, can rapidly search for high-performing neural architectures against diverse perturbations. Specifically, CRoZe evaluates the network’s robustness in a single step based on the consistency across the features (z and z^r), parameters (θ and θ^r), and gradients ($\nabla_{\theta} \mathcal{L}$ and $\nabla_{\theta^r} \mathcal{L}$) between clean and robust network against clean and perturbed inputs, respectively.

To tackle this challenge, we propose a novel and lightweight **Robust Zero-cost proxy (CRoZe)** that can rapidly evaluate the robustness of the neural architectures against *diverse semantic-preserving* perturbations without requiring any iterative training. While prior clean zero-shot NAS methods (Abdelfattah et al., 2021; Mellor et al., 2021) introduced proxies that score the networks with randomly initialized parameters (Lee et al., 2019; Wang et al., 2020; Liu et al., 2021; Tanaka et al., 2020) without any training, they only consider which parameters are highly sensitive to clean inputs for a given task, as determined by measuring the scale of the gradients based on the objectives and thus yield networks that are vulnerable against perturbed inputs (Figure 1a).

Specifically, our proxy captures the consistency across the features, parameters, and gradients of a randomly initialized model for both clean and perturbed inputs, which is updated with a single gradient step (Figure 1b). This metric design measures the model’s robustness in multiple aspects, which is indicative of its generalized robustness to diverse types of perturbations. This prevents the metric from being biased toward a specific type of perturbation and ensures its robustness across diverse semantic-preserving perturbations. Empirically, we find that a neural architecture with the highest performance for a single type of perturbation tends to exhibit larger feature variance for other types of perturbations (Figure 4), while our proxy that considers the robustness in multiple aspects obtains features with smaller variance even on diverse types of perturbations. This suggests that our proxy is able to effectively discover architectures with enhanced generalized robustness.

We validate our approach through extensive experiments on diverse search spaces (NAS-Bench 201, DARTS) and multiple datasets (CIFAR-10, CIFAR-100, ImageNet16-120), with not only the adversarial perturbations but also with various types of common corruptions (Hendrycks and Dietterich, 2019), against both clean zero-shot NAS (Abdelfattah et al., 2021; Mellor et al., 2021) and robust NAS baselines (Mok et al., 2021; Guo et al., 2020). The experimental results clearly demonstrate our method’s effectiveness in finding generalizable robust neural architectures, as well as its computational efficiency. Our contributions can be summarized as follows:

- We propose a simple yet effective consistency-based zero-cost proxy for robust NAS against diverse perturbations via measuring the consistency of features, parameters, and gradients between perturbed and clean samples.
- Our approach can rapidly search for generalizable neural architectures that do not perform well only on clean samples but also are highly robust against diverse types of perturbations on various datasets.

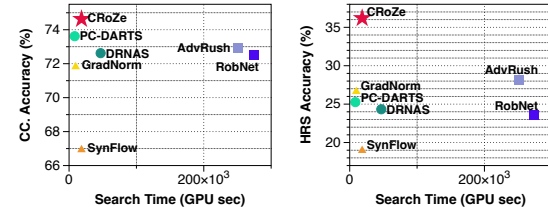


Figure 2: Final performance of the searched network in DARTS search space on CIFAR-10 through **clean one-shot NAS, robust NAS, clean zero-shot NAS and our CRoZe.**

- Our proxy obtains superior Spearman’s ρ across benchmarks compared to existing clean zero-shot NAS methods and identifies robust architectures that exceed robust NAS frameworks by **6.21%** with **14.7 times less search cost** within the DARTS search space on CIFAR-10.

2 RELATED WORK

Robustness of DNNs against Perturbations. Despite the recent advances, deep neural networks (DNNs) are still vulnerable to small perturbations on the input, e.g., common corruptions (Hendrycks and Dietterich, 2019), random noises (Dodge and Karam, 2017), and adversarial perturbations (Biggio et al., 2013; Szegedy et al., 2014), which can result in incorrect predictions with high confidence. To overcome such vulnerability against diverse perturbations, many approaches have been proposed to train the neural network to be robust against each type of perturbation individually. To learn a rich visual representation from limited crawled data, previous works (Hendrycks et al., 2020; Cubuk et al., 2020) utilized a combination of strong data augmentation functions to improve robustness to common corruptions and random Gaussian noises. Furthermore, to overcome adversarial vulnerability, widely used defense mechanisms (Goodfellow et al., 2015; Madry et al., 2018; Moosavi-Dezfooli et al., 2016) generate adversarially perturbed images by taking multiple gradient steps to maximize the training loss and use them in training to improve the model’s robustness.

Neural Architecture Search. Neural architecture search (NAS) leverages reinforcement learning (Zoph and Le, 2017; Baker et al., 2017; Zhong et al., 2018) or evolutionary algorithms (Real et al., 2017; Liu et al., 2018b; Elsken et al., 2019; Real et al., 2019) to automate the design of optimal architectures for specific tasks or devices. However, those are computationally intensive, making them impractical to be applied in real-world applications. To address this, zero-shot NAS methods (Abdelfattah et al., 2021; Mellor et al., 2021) have emerged that significantly reduce search costs by predicting the performance of architecture at the initialization state only with a single batch of a given dataset. Despite the improvement in NAS, previous zero-shot NAS methods, and conventional NAS methods aim only to find architectures with high accuracy on clean examples, without considering their robustness against various perturbations. In particular, SynFlow (Abdelfattah et al., 2021) lacks data incorporation in its scoring mechanism, potentially failing to find the network that can handle diverse perturbations. NASWOT (Mellor et al., 2021) search models with low activation correlation across two different inputs, emphasizing their distinguishability. However, the criterion contradicts the requirements of robustness, which necessitates finding a network that maintains similar activations for both clean and perturbed inputs. As a result, models found with previous NAS methods often lead to incorrect predictions with high confidence (Mok et al., 2021; Jung et al., 2023) even with small imperceptible perturbations applied to the inputs. A new class of NAS methods (Guo et al., 2020; Mok et al., 2021) that considers robustness against adversarial perturbations has emerged. Yet, they require adversarial training of the supernet, which demands more computational resources than conventional NAS (Real et al., 2017; Elsken et al., 2019) due to repeated adversarial gradient steps. Furthermore, adversarial robust NAS often overfit to a single type of perturbation due to only considering the adversarial robustness. Thus, there is a need for a lightweight NAS approach that can achieve generalized robustness for safe real-world applications.

3 METHODS

Our ultimate goal is to efficiently search for robust architectures that have high performance on various tasks, regardless of the type of perturbations applied to the input samples. To achieve this goal, we propose a Consistency-based Robust Zero-cost proxy (**CRoZe**) that considers the consistency of the features, parameters, and gradients between a single batch of clean and perturbed inputs obtained by taking a single gradient step. The proposed proxy enables the rapid evaluation of the robustness of the neural architectures in the random states, without any adversarial training (Figure 1).

3.1 ROBUST ARCHITECTURES

Formally, our goal is to accurately estimate the final robustness of a given neural architecture \mathcal{A} with given a single batch of inputs $B = \{(x, y)\}$, without training. Here, $x \in X$ is the input sample, and $y \in Y$ is its corresponding label for given dataset $\mathcal{D} = \{X, Y\}$. In the following section, the network

$f_\theta(\cdot)$ consists of an encoder $e_\psi(\cdot)$ and a linear layer $h_\pi(\cdot)$, which is \mathcal{A} that is parameterized with ψ and π , respectively. The most straightforward approach to evaluate the robustness of the network is measuring the accuracy against the perturbed input x' with unseen semantic-preserving perturbations, as follows:

$$\text{Accuracy} = \frac{1}{N} \sum_{n=1}^N \zeta(\arg \max_{c \in Y} \mathbb{P}(h_\pi \circ e_\psi(x') = c) = y), \quad (1)$$

where ζ is the Kronecker delta function, which returns 1 if the predicted class c is the same as y , and 0 otherwise, x' is a perturbed input, such as one with random Gaussian noise, common types of corruptions (Hendrycks et al., 2020), or adversarial perturbations (Madry et al., 2018; Goodfellow et al., 2015) applied to it. Specifically, to have a correct prediction on the unseen perturbed input x' , the model needs to extract similar features between x' and x , assuming that the model can correctly predict the label for input x as follows:

$$\|e_\psi(x) - e_\psi(x')\| \leq \epsilon, \quad (2)$$

where ϵ is sufficiently small bound. Thus, a robust model is one that can extract consistent features across a wide range of perturbations. However, precisely assessing the accuracy of the model against perturbed inputs requires training from scratch with a full dataset, which incurs a linear increase in the computational cost with respect to the number of neural architectures to be evaluated.

3.2 ESTIMATING ROBUST NETWORK THROUGH PERTURBATION

In this section, we explain details on preliminary protocols before computing our proxy. Due to the impractical computation cost to obtain a combinatorial number of fully-trained models in a given neural architecture search space (i.e., 10^{19} for DARTS), we propose to utilize two surrogate networks which together can estimate the robustness of fully-trained networks within a single gradient step. The two surrogate networks are a clean network f_θ with the randomly initialized parameter θ and a robust network f_{θ^r} with the robust parameter θ^r , which is determined with a parameter perturbations from f_θ . Then, the obtained θ^r is used to generate the single batch of perturbed inputs for our proxy.

Robust Parameter Update via Layer-wise Parameter Perturbation. We employ a surrogate robust network to estimate the output of fully-trained networks against perturbed inputs. To make the perturbation stronger, we use a double-perturbation scheme that combines layer-wise parameter perturbations (Wu et al., 2020) and input perturbations, both of which maximize the training objectives \mathcal{L} . This layer-wise perturbation allows us to learn smoother updated parameters by min-max optimization, through which we can obtain the model with the maximal possible generalization capability (Wu et al., 2020; Foret et al., 2021) within a single step. Specifically, given a network f is composed of M layers, $f_\theta = f_{\theta_M} \circ \dots \circ f_{\theta_1}$, with parameters $\theta = \{\theta_1, \dots, \theta_M\}$, the m^{th} layer-wise parameter perturbation is done as follows:

$$\theta_m^r \leftarrow \theta_m + \beta * \frac{\nabla_{\theta_m} \mathcal{L}(f_\theta(x), y)}{\|\nabla_{\theta_m} \mathcal{L}(f_\theta(x), y)\|} * \|\theta_m\|, \quad (3)$$

where β is the step size for parameter perturbations, $\|\cdot\|$ is the norm, and \mathcal{L} is the cross-entropy objective. This bounds the size of the perturbation by the norm of the original parameter $\|\theta_m\|$.

Perturbed Input. On top of the perturbed parameters (Eq. 3), we generate perturbed input images by employing fast gradient sign method (FGSM) (Goodfellow et al., 2015), which is the worst case adversarial perturbation to the input x as follows:

$$\delta = \epsilon \text{sign}(\nabla_x \mathcal{L}(f_{\theta^r}(x), y)), \quad (4)$$

where δ is a generated adversarial perturbation that maximizes the cross-entropy objective \mathcal{L} of given input x and given label y . Then, we utilize the perturbed inputs ($x' = x + \delta$) to estimate the robustness of the fully-trained model. Although CRoZe is input perturbation-agnostic proxy (Table 4), we employ adversarially perturbed inputs for all the following sections.

3.3 CONSISTENCY-BASED PROXY FOR ROBUST NAS

We now elaborate the details on our proxy that evaluate the robustness of the architecture with the two surrogate networks: the clean network that is randomly initialized and uses clean images x as inputs, and the robust network parameterized with θ^r which uses perturbed images $x + \delta$ as inputs.

Features, Parameters, and Gradients. As we described in Section 3.1, we first evaluate the representational consistency between clean input (x) and perturbed input (x') by forwarding them through the encoder of clean surrogate network $f_\theta(\cdot)$ and robust surrogate network $f_{\theta^r}(\cdot)$, respectively, as follows:

$$\mathcal{Z}_m(f_\theta(x), f_{\theta^r}(x')) = 1 + \frac{z_m \cdot z_m^r}{\|z_m\| \|z_m^r\|}, \quad (5)$$

where z_m and z_m^r are output feature of each network $f_\theta(\cdot)$ and $f_{\theta^r}(\cdot)$, respectively, from each m^{th} layer. Especially, we measure layer-wise consistency with cosine similarity function between clean and robust features. The higher feature consistency infers the higher robustness of the network.

However, the proxy solely considering the feature consistency within a single batch can be heavily reliant on the selection of the batch. Therefore, to complement the feature consistency, we propose incorporating the consistency of updated parameters and gradient conflicts from each surrogate network as additional measures to evaluate the robustness of the network. To introduce these concepts, let us first denote the gradient and updated parameter of each surrogate network. The gradient g from the clean surrogate network f_θ and robust surrogate network f_{θ^r} against clean images x and perturbed images x' , respectively, are obtained as follows:

$$g = \nabla_\theta \mathcal{L}(f_\theta(x), y), \quad g^r = \nabla_{\theta^r} \mathcal{L}(f_{\theta^r}(x'), y), \quad (6)$$

where g and g^r are the gradients with respect to cross-entropy objectives \mathcal{L} of the clean images x and perturbed images $x' = x + \delta$, respectively. Then, we can acquire the single-step updated clean parameters θ and robust parameters θ^r calculated with gradients g and g^r and learning rate γ , respectively as follows:

$$\theta_1 \leftarrow \theta - \gamma g, \quad \theta_1^r \leftarrow \theta^r - \gamma g^r. \quad (7)$$

Since each surrogate network represents the model for each task, i.e., clean classification and perturbed classification, the parameters and gradients of each surrogate network correspond to the updated weights and convergence directions for each task. Thus, the network that has high robustness will exhibit identical or similar parameter spaces for both classification tasks. However, as acquiring parameters of a fully-trained network is impractical, we estimate the converged parameters with the single-step updated parameters θ_1 and θ_1^r . Accordingly, since the higher similarity of single-step updated parameters may promote the model to converge to an identical or similar parameter space for both tasks, we evaluate the parameter similarity as one of our proxy terms as follows:

$$\mathcal{P}_m(\theta_1, \theta_1^r) = 1 + \frac{\theta_{1,m} \cdot \theta_{1,m}^r}{\|\theta_{1,m}\| \|\theta_{1,m}^r\|}. \quad (8)$$

Furthermore, each gradient of the surrogate networks represents the converged direction of given objectives for each task, which is cross-entropy loss of clean input and perturbed input (Eq. 6). Thus, we employ the gradients similarity as an evaluation of the difficulties of optimizing architecture for both tasks. Therefore, when the gradient directions are highly aligned between the two tasks, the learning trajectory for both tasks becomes more predictable, facilitating the optimization of both tasks easily. In contrast, orthogonal gradient directions lead to greater unpredictability, hindering optimization and potentially resulting in suboptimality for both clean or perturbed classification tasks. Therefore, to evaluate the stability of optimizing both tasks, we measure the absolute value of gradient similarity as follows:

$$\mathcal{G}_m(g, g^r) = \left| \frac{g_m \cdot g_m^r}{\|g_m\| \|g_m^r\|} \right|. \quad (9)$$

Consistency-based Robust Zero-Cost Proxy: CRoZe. In sum, to evaluate the robustness of the given architecture, we propose a scoring mechanism that evaluates the similarities of features, parameters, and gradients between the clean network f_θ and the robust network f_{θ^r} that are obtained with a single gradient update. Therefore, the robustness score for a given neural architecture is computed as follows:

$$\text{CRoZe}(x, x'; f_\theta, f_{\theta^r}) = \sum_{m=1}^M \mathcal{Z}_m \times \mathcal{P}_m \times \mathcal{G}_m. \quad (10)$$

That is, we score the network f_θ with a higher CRoZe score as more robust to perturbations. In the next section, we show that this measure is highly correlated with the actual robustness of a fully-trained model (Table 1a).

4 EXPERIMENTS

We now experimentally validate our proxy designed to identify robust architectures that perform well on both clean and perturbed inputs, on multiple benchmarks. We first evaluate Spearman’s ρ between robust performance and the proxy’s values across different tasks and perturbations in the NAS-Bench-201 search space, comparing it to clean zero-shot NAS methods (Section 4.2). We then evaluate the computational efficiency and final performance of the chosen architecture using our proxy in the DARTS search space, comparing it to existing robust NAS methods, which are computationally costly (Section 4.3). Lastly, we analyze the proxy’s ability to accurately reflect the fully trained model’s behavior in a single step, as well as the capacity of the chosen robust architecture to consistently generate features, aligned gradients, and parameters against clean and perturbed inputs (Section 4.4).

4.1 EXPERIMENTAL SETTING

Baselines. We consider three types of existing NAS approaches as our baselines. **1) Clean one-shot NAS** (Xu et al., 2020; Chen et al., 2020) One-shot NAS methods for searching architectures only on clean samples. **2) Clean zero-shot NAS** (Abdelfattah et al., 2021; Mellor et al., 2021): Zero-shot NAS with proxies that evaluate the clean performance of architectures without any training. **3) Robust NAS** (Guo et al., 2020; Mok et al., 2021) One-shot NAS methods for searching architectures only on adversarially perturbed samples.

Datasets. For the NAS-Bench-201 (Dong and Yang, 2019; Jung et al., 2023) search space, we validate our proxy across different tasks (CIFAR-10, CIFAR-100, and ImageNet16-120) and perturbations (FGSM (Goodfellow et al., 2015), PGD (Madry et al., 2018), and 15 types of common corruptions (Hendrycks and Dietterich, 2019)). To measure Spearman’s ρ between final accuracies and our proxy values, we use both clean NAS-Bench-201 (Dong and Yang, 2019) and robust NAS-Bench-201 (Jung et al., 2023), which include clean accuracies and robust accuracies. Finally, we search for the optimal architectures with our proxy in DARTS (Liu et al., 2019) search space and compare the final accuracies against previous NAS methods (Mok et al., 2021; Guo et al., 2020; Chen et al., 2020; Abdelfattah et al., 2021) on CIFAR-10 and CIFAR-100.

Standard Training & Adversarial Training. For a fair comparison, we use the same training and testing settings to evaluate all the architectures searched with all NAS methods, including ours. **1) Standard Training:** We train the neural architectures for 200 epochs under SGD optimizer with a learning rate of 0.1 and weight decay $1e-4$, and use a batch size of 64 following (Mok et al., 2021). **2) Adversarial Training:** We adversarially train the searched neural architectures with l_∞ PGD attacks with the epsilon of $8/255$, step size $2/255$, and 7 steps. We evaluate the robustness against various perturbations, which are FGSM Goodfellow et al. (2015), PGD Madry et al. (2018), and common corruptions Hendrycks and Dietterich (2019). All attacks utilized in evaluation are l_∞ attacks with the epsilon of $8/255$. More experimental details are described in Supplementary A.

4.2 RESULTS ON NAS-BENCH-201

Standard-Trained Neural Architectures. In order to verify the effectiveness of our proxy in searching for high-performing neural architectures across various tasks and perturbations, we conduct experiments using Spearman’s ρ as a metric to evaluate the preservation of the rank between the proxy values and final accuracies (Abdelfattah et al., 2021; Mellor et al., 2021; Dong et al., 2023). For Spearman’s ρ between clean accuracies and proxy values, existing clean zero-shot NAS works (Abdelfattah et al., 2021; Mellor et al., 2021) performed worse than using the number of parameters as a proxy (#Params.). In contrast, our proxy shows significantly higher correlations with clean accuracies across all tasks, demonstrating improvements of 10.2% and 9.31% on CIFAR-10 and CIFAR-100, respectively, compared to best-performing baselines (Table 1a, 2).

Furthermore, CRoZe shows remarkable Spearman’s ρ for robust accuracies obtained against adversarial perturbations and corrupted noises across tasks. Notably, our proxy outperforms the SynFlow (Abdelfattah et al., 2021) by 6.73% and 9.05% in an average of Spearman’s ρ for adversarial perturbations and common corruptions on CIFAR-10, respectively (Table 1a). Our results on multiple benchmark tasks with diverse perturbations highlight the ability of our proxy to effectively search for

Table 1: Comparison of Spearman’s ρ between the actual accuracies and the proxy values on CIFAR-10 in the NAS-Bench-201 search space. Plain, Grasp, Fisher, GradNorm, and SynFlow are zero-shot NAS methods from Abdelfattah et al. (2021). NASWOT Mellor et al. (2021) is using activation as a proxy. Clean stands for clean accuracy and robust accuracies are evaluated against adversarial perturbations Goodfellow et al. (2015) with various attack sizes (ϵ) and common corruptions (Hendrycks and Dietterich, 2019). Avg. stands for average Spearman’s ρ values with all accuracies. **Bold** and underline stands for the best and second.

Proxy Type	Clean	Adversarial Perturbation			Common Corruption					Proxy Type	Clean	FGSM	PGD	HRS(FGSM)	HRS(PGD)
		$\epsilon = 8$	$\epsilon = 4$	$\epsilon = 2$	Weather	Noise	Blur	Digital	Avg.						
FLOPs	0.726	0.753	0.740	0.716	0.665	0.138	0.219	0.473	0.554	FLOPs	0.670	0.330	0.418	0.531	0.515
#Params.	<u>0.747</u>	0.756	0.739	0.713	<u>0.674</u>	0.131	0.215	0.489	0.558	#Params.	<u>0.678</u>	0.341	<u>0.429</u>	<u>0.541</u>	<u>0.526</u>
Plain	-0.073	-0.059	-0.055	-0.029	-0.041	0.048	0.035	-0.032	-0.026	Plain	-0.042	-0.007	-0.012	-0.016	-0.016
Grasp	0.440	0.547	0.563	0.541	0.459	0.217	0.164	0.327	0.407	Grasp	0.470	0.324	0.341	0.392	0.375
Fisher	0.356	0.457	0.491	0.498	0.407	<u>0.217</u>	0.221	0.240	0.361	Fisher	0.482	0.226	0.276	0.335	0.334
GradNorm	0.598	0.750	0.766	0.743	0.641	0.246	0.227	0.423	0.549	GradNorm	0.659	0.336	0.400	0.490	0.478
SynFlow	0.737	<u>0.728</u>	0.750	0.727	0.673	0.188	0.165	0.554	<u>0.572</u>	SynFlow	0.635	<u>0.355</u>	0.420	0.519	0.498
NASWOT	0.660	0.511	0.507	0.435	0.466	-0.066	-0.005	0.413	0.365	NASWOT	0.600	0.332	0.381	0.437	0.438
CRoZe	0.823	0.826	0.801	0.780	0.743	0.190	0.224	0.566	0.619	CRoZe	0.723	0.417	0.501	0.602	0.588

(a) Standard-Trained

(b) Adversarially-Trained

Table 2: Comparison of Spearman’s ρ between the actual accuracies and the proxy values on CIFAR-100 and ImageNet16-120 in NAS-Bench-201 search space. Avg. stands for average Spearman’s ρ values with all accuracies within each task. **Bold** and underline stands for the best and second.

Proxy Type	CIFAR-100							ImageNet16-120		
	Clean	FGSM	Weather	Noise	Blur	Digital	Avg.	Clean	FGSM	Avg.
FLOPs	0.705	0.663	0.674	0.25	0.444	0.607	0.557	0.657	0.611	0.634
#Params.	0.720	0.654	0.685	0.240	0.438	0.618	0.559	0.683	0.627	0.655
Plain Abdelfattah et al. (2021)	-0.126	-0.100	-0.095	-0.002	-0.064	-0.080	-0.078	-0.15	-0.145	-0.148
Grasp Abdelfattah et al. (2021)	0.475	0.548	0.486	<u>0.262</u>	0.374	0.441	0.431	0.400	0.437	0.419
Fisher Abdelfattah et al. (2021)	0.378	0.573	0.419	0.325	0.435	0.391	0.420	0.315	0.388	0.352
GradNorm Abdelfattah et al. (2021)	0.635	0.791	0.549	0.358	0.534	0.609	<u>0.579</u>	0.562	0.643	0.603
SynFlow Abdelfattah et al. (2021)	0.769	0.685	<u>0.703</u>	0.217	0.389	<u>0.642</u>	0.568	<u>0.751</u>	<u>0.695</u>	<u>0.723</u>
NASWOT Mellor et al. (2021)	0.683	0.513	0.353	0.273	0.517	0.000	0.390	0.653	0.686	0.670
CRoZe	0.787	<u>0.693</u>	0.747	0.251	<u>0.450</u>	0.682	0.602	0.769	0.696	0.733

robust architectures that can make consistently outperform predictions against various perturbations. Importantly, our proxy is designed to prioritize generalizability, and as a result, it exhibits consistently enhanced correlation with final accuracies for both clean and perturbed samples. This result indicates that considering generalization ability is effective in identifying robust neural architectures against diverse perturbations but also leads to improved performance for clean neural architectures.

Adversarially-Trained Neural Architectures. We also validate the ability of our proxy to precisely predict the robustness of adversarially-trained networks, specifically for adversarial perturbations. Adversarial training (Madry et al., 2018) is a straightforward approach to achieve robustness in the presence of adversarial perturbations. To assess the Spearman’s ρ of robustness in adversarially-trained networks, we construct a dataset consisting of final robust accuracies of 500 randomly sampled neural architectures from NAS-Bench-201 search space that are adversarially-trained (Madry et al., 2018) from scratch.

Considering the trade-off between the clean and robust accuracy in adversarial training (Zhang et al., 2019), we employ the harmonic robustness score (HRS) (Devaguptapu et al., 2021) to evaluate the overall performance of the adversarially-trained models. When comparing the correlations between clean performances and proxy values, existing clean zero-shot NAS approaches, i.e., SynFlow and Grasp, demonstrate higher correlations in the FGSM or PGD, but their correlations with clean performances are poorer than GradNorm and Fisher, respectively. This result shows that clean zero-shot NAS methods tend to search for architectures that are more prone to overfitting to either clean or robust tasks (Table 1b). In contrast, CRoZe consistently achieves higher Spearman’s ρ for both clean and robust tasks, ultimately enabling the search for architecture with high HRS due to consideration of alignment in gradients.

4.3 END-TO-END GENERALIZATION PERFORMANCE ON DARTS

In this section, we evaluate the effectiveness of CRoZe in rapidly searching for generalized neural architectures in the DARTS search space and compare it with previous clean one-shot NAS (Xu et al., 2020; Chen et al., 2020), clean zero-shot NAS (Tanaka et al., 2020), and robust NAS (Mok et al., 2021; Guo et al., 2020) in terms of performance and computational cost.

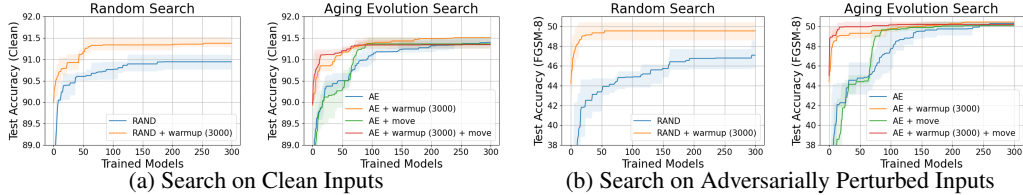


Figure 3: Search with our proxy on CIFAR-10 in NAS-Bench-201 search space. Our proxy can reduce the sampling costs in searching for neural architectures against both clean (left) and perturbed samples (right).

Efficient Sampling with CRoZe. The efficiency of our proxy lies in its ability to evaluate neural architectures without iteratively training the models with those architectures. As a result, the majority of the search time is dedicated to the sampling of candidate architectures. To thoroughly explore the sampling costs involved in using our proxy to identify good neural architectures, we conduct experiments in the NAS-Bench-201 search space with two representative sampling-based search algorithms: random search (RAND) and evolutionary search (AE).

Our experiments show that CRoZe can rapidly identify an architecture with 91.5% clean accuracy and 50% robust accuracy against FGSM attacks, even at the initial stages of the search. By leveraging the initial pool of architectures with high proxy values obtained from CRoZe (RAND+warmup and AE+warmup), our proxy effectively reduces the sampling costs and rapidly identifies high-performing architectures for clean inputs (Figure 3a). Moreover, by focusing sampling around the architecture with the highest proxy values of CRoZe (AE+warmup+move), we can search for architecture with even better robust performance using a less number of sampled models (< 50) (Figure 3b). Overall, our results highlight the effectiveness of CRoZe in searching for high-performing neural architectures against both clean and perturbed inputs in the NAS-Bench-201 search space.

End-to-End Performance. We validate the final performance of the neural architectures discovered by CRoZe (Table 3) and compare the search time and performance with existing NAS frameworks including robust NAS (RobNet (Guo et al., 2020) and AdvRush (Mok et al., 2021)), clean zero-shot NAS (SynFlow, GradNorm (Abdelfattah et al., 2021)), and clean one-shot NAS (PC-DARTS (Xu et al., 2020) and DrNAS (Chen et al., 2020)). For a fair comparison between clean zero-shot NAS (SynFlow, GradNorm) and CRoZe, we sample the same number (5,000) of candidate architectures using the warmup+move strategy in the DARTS search space. All experiments are conducted on a single NVIDIA 3090 RTX GPU to measure search costs.

Our proxy surpasses the robust NAS methods, RobNet and AdvRush, in terms of robust accuracy against FGSM on CIFAR-10, achieving improvements of 8.95% and 6.21%, respectively. Notably, CRoZe also shows the highest HRS accuracy with an 8.56% increase compared to AdvRush on CIFAR-10, indicating that the neural architectures discovered by CRoZe effectively mitigate the trade-off between clean and robust accuracy, even with 14.7 times reduced search cost. When compared to the previously best-performing clean zero-cost proxy, SynFlow, CRoZe finds architectures with significantly superior performance across clean, common corruptions, and FGSM scenarios, showcasing the effectiveness of our proxy in identifying generalized architectures. Additionally, the neural architecture chosen by CRoZe outperforms clean one-shot NAS approaches in HRS accuracy, effectively addressing diverse perturbations and clean inputs (Figure 2).

4.4 FURTHER ANALYSIS

Feature Variance of the Robust Models. Our proxy searches for architectures that can generalize to all types of perturbed inputs, which are not overfitted to a single type of perturbation, as described in Section 3.1 (Eq. 2). To validate this, we analyzed the feature variance of neural architectures that demonstrated the highest performance against a single type of perturbation, namely FGSM and PGD, compared to an architecture selected with the CRoZe proxy from a pool of 300 standard-trained and adversarially-trained models. Features were obtained from 18 different perturbations, including clean, PGD, FGSM, and 15 types of common corruptions. Remarkably, the neural architectures selected with our proxy exhibited the smallest standard deviations between

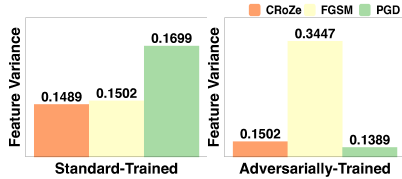


Figure 4: Feature variance across diverse perturbations.

Features were obtained from 18 different perturbations, including clean, PGD, FGSM, and 15 types of common corruptions. Remarkably, the neural architectures selected with our proxy exhibited the smallest standard deviations between

Table 3: Comparisons of the final performance and search time of the searched network in DARTS search space on CIFAR-10 and CIFAR-100. All NAS methods are executed on a single NVIDIA 3090 RTX GPU.

Task	NAS Method	NAS Training-free	Params (M)	Search Time (GPU sec)	Standard-Trained			
					Clean	CC.	FGSM	HRS
CIFAR-10	PC-DARTS (Xu et al., 2020)		3.60	8355	95.35	73.62	14.56	25.26
	DrNAS (Chen et al., 2020)		4.10	46857	94.64	72.62	13.96	24.33
	RobNet (Guo et al., 2020)		5.44	274062	95.30	72.51	13.43	23.54
	AdvRush (Mok et al., 2021)		4.20	251245	94.80	72.00	16.17	27.63
	GradNorm (Abdelfattah et al., 2021)	✓	4.69	9740	92.84	71.82	15.55	26.64
	SynFlow (Abdelfattah et al., 2021)	✓	5.08	10138	90.41	66.93	10.59	18.96
	CRoZe	✓	5.52	17066	94.45	74.63	22.38	36.19
CIFAR-100	PC-DARTS (Xu et al., 2020)		3.60	8355	76.96	49.95	7.93	14.38
	DrNAS (Chen et al., 2020)		4.10	46857	77.46	50.76	7.87	14.29
	RobNet (Guo et al., 2020)		5.44	274062	76.15	49.43	6.47	11.93
	AdvRush (Mok et al., 2021)		4.20	251245	76.33	49.53	8.21	14.83
	GradNorm (Abdelfattah et al., 2021)	✓	3.83	9554	67.95	42.81	5.11	9.51
	SynFlow (Abdelfattah et al., 2021)	✓	4.42	9776	75.93	48.53	8.22	14.83
	CRoZe	✓	4.72	17457	75.18	49.35	10.84	18.95

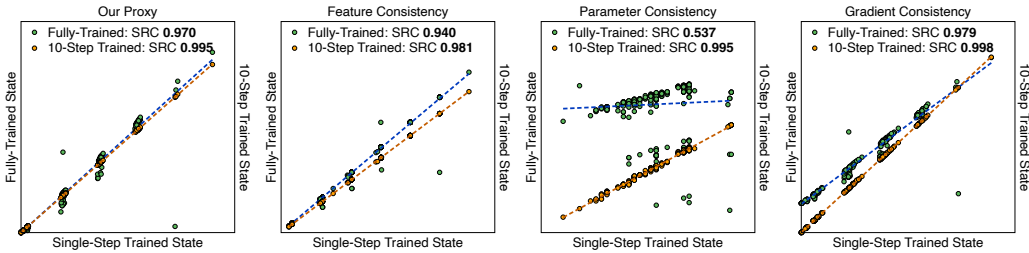


Figure 5: Spearman’s ρ in our proxy and each consistency component between the neural architectures with single-step trained states and two different states, which are fully-trained and 10-step trained states, respectively, against clean and perturbed images.

the features obtained from the 18 different perturbations, in both standard and adversarially-trained scenarios. Conversely, the architecture with the best PGD robustness demonstrated 2.48 times larger variations, indicating a higher risk of overfitting to specific perturbations. These results provide compelling evidence of the effectiveness of CRoZe in identifying robust architectures that can consistently extract features and generalize across diverse perturbations.

Generalization to Diverse Perturbations. CRoZe evaluates the consistency between clean and perturbed inputs, regardless of the perturbation type, under the assumption that perturbed inputs retain the same semantic information as clean inputs. To empirically demonstrate the independence of our proxy from specific perturbation types, we introduce random Gaussian noise in place of adversarial perturbations in Eq. 4. As evidenced in Table 4, CRoZe consistently exhibits similar Spearman’s ρ in the NAS-Bench-201 search space. This emphasizes that CRoZe captures the characteristics of robust architectures through the consistency of clean and perturbed inputs, irrespective of the perturbation types employed.

Type	Standard-Trained				
	Clean	CC.	FGSM ($\epsilon, 8$)	FGSM ($\epsilon, 4$)	FGSM ($\epsilon, 2$)
Gaussian Noise	0.810	0.436	0.821	0.797	0.778
Adversarial	0.823	0.436	0.823	0.826	0.801
	Adversarially-Trained				
	Clean	PGD	HRS(PGD)	FGSM ($\epsilon, 8$)	HRS(FGSM)
Gaussian Noise	0.718	0.503	0.590	0.415	0.603
Adversarial	0.723	0.501	0.588	0.417	0.602

Table 4: Comparisons of perturbation type in CRoZe.

Assessment of CRoZe Predictiveness. To empirically validate whether our proxy obtained from a random state accurately represents the proxy in the fully-trained model, we conducted an analysis using Spearman’s ρ . We randomly sampled 300 architectures from the NAS-Bench-201 search space and trained them on the entire dataset, using both the full training and reduced training only of 10 steps. The Spearman’s ρ between the proxy value obtained from a single-step trained state and the 10-step trained state shows a strong correlation of 0.995. Even after full training, the correlation remained high at 0.970 (Figure 5). These suggest that our proxy, derived from estimated surrogate networks, can significantly reduce the computational costs associated with obtaining fully-trained models. Furthermore, each component of CRoZe consistently demonstrates a high correlation with the fully-trained states, supporting the notion that the high correlation computed with the final state is not solely a result of the collective influence of components, but rather an accurate estimation.

Validation of CRoZe for Estimating Fully-Trained Neural Architectures. To investigate whether the architectures selected with our proxy possess the desired robustness properties discussed in Section 3.1, we conduct a comprehensive analysis. From a pool of 300 samples in the NAS-Bench-201 search space, we select the top-5 and bottom-5 neural architectures based on our proxy values, excluding those with a robust accuracy of less than 20%.

We evaluate the performances of these architectures that are standard-trained and adversarially-trained against clean inputs and three distinct types of perturbed inputs: adversarial perturbations (i.e., FGSM and PGD), and common corruptions. Notably, the top-5 networks show impressive average clean accuracies of 89.62%, 84.36% on CIFAR-10, while the bottom-5 networks achieve significantly lower average clean accuracies of 61.34%, 51.64% in standard training and adversarial training, respectively (Table 5). Moreover, the top-5 networks exhibit an average robust accuracy of 54.95% against perturbations, compared to only 28.50% for the bottom-5 group. Furthermore, by considering feature consistency between clean and perturbed inputs, as defined in Eq. 2, the top-5 group exhibited similar features, whereas the bottom-5 group showed dissimilar features (Figure 6). This supports that architectures with consistent features across inputs are more likely to make accurate predictions under perturbations. Overall, our analysis provides strong evidence that our proxy can search for generalizable robust architectures that accurately predict the final accuracies under diverse perturbations.

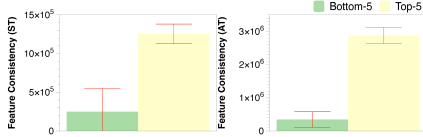


Figure 6: Comparisons of feature consistency in fully-trained states.

We evaluate the performances of these architectures that are standard-trained and adversarially-trained against clean inputs and three distinct types of perturbed inputs: adversarial perturbations (i.e., FGSM and PGD), and common corruptions.

Type	Standard Trained (ST)				
	Clean	CC.	PGD	FGSM	Avg. Rob.
Top-5	89.62	77.68	26.09	61.08	54.95
Bottom-5	61.34	49.13	19.35	17.01	28.50
Type	Adversarially Trained (AT)				
	Clean	PGD	HRS(PGD)	FGSM	HRS(FGSM)
Top-5	84.36	40.55	54.76	66.48	74.34
Bottom-5	51.64	22.59	31.36	37.20	43.04

Table 5: Comparisons of the performance. Table 5: Comparisons of the performance. Table 5: Comparisons of the performance. Table 5: Comparisons of the performance. Table 5: Comparisons of the performance.

5 CONCLUSION

While neural architecture search (NAS) is a powerful technique for automatically discovering high-performing deep learning models, previous NAS works suffer from two major drawbacks: computational inefficiency and compromised robustness against diverse perturbations, which hinder their applications in real-world scenarios with safety-critical applications. In this paper, we proposed a simple yet effective lightweight robust NAS framework that can rapidly search for well-generalized neural architectures against diverse tasks and perturbations. To this end, we proposed a novel consistency-based zero-cost proxy that evaluates the robustness of randomly initialized neural networks by measuring the consistency in their features, parameters, and gradients for both clean and perturbed inputs. Experimental results demonstrate the effectiveness of our approach in discovering well-generalized architectures across diverse search spaces, multiple datasets, and various types of perturbations, outperforming the baselines with significantly reduced search costs. Such simplicity and effectiveness of our approach open up new possibilities for automatically discovering high-performing models that are well-suited for safety-critical applications.

REFERENCES

- Mohamed S Abdelfattah, Abhinav Mehrotra, Łukasz Dudziak, and Nicholas D Lane. Zero-cost proxies for lightweight nas. *International Conference on Learning Representations*, 2021.
- Bowen Baker, Otkrist Gupta, Nikhil Naik, and Ramesh Raskar. Designing neural network architectures using reinforcement learning. In *International Conference on Learning Representations*, 2017.
- Battista Biggio, Iginio Corona, Davide Maiorca, Blaine Nelson, Nedim Šrđić, Pavel Laskov, Giorgio Giacinto, and Fabio Roli. Evasion attacks against machine learning at test time. In *Joint European conference on machine learning and knowledge discovery in databases*, pages 387–402. Springer, 2013.
- Han Cai, Chuang Gan, Tianzhe Wang, Zhekai Zhang, and Song Han. Once-for-all: Train one network and specialize it for efficient deployment. *International Conference on Learning Representations*, 2019.
- Xiangning Chen, Ruochen Wang, Minhao Cheng, Xiaocheng Tang, and Cho-Jui Hsieh. Drnas: Dirichlet neural architecture search. *arXiv preprint arXiv:2006.10355*, 2020.
- Ekin D Cubuk, Barret Zoph, Jonathon Shlens, and Quoc V Le. Randaugment: Practical automated data augmentation with a reduced search space. In *Advances in Neural Information Processing Systems*, 2020.
- Chaitanya Devaguptapu, Devansh Agarwal, Gaurav Mittal, Pulkit Gopalani, and Vineeth N Balasubramanian. On adversarial robustness: A neural architecture search perspective. In *IEEE International Conference on Computer Vision*, pages 152–161, 2021.
- Samuel Dodge and Lina Karam. A study and comparison of human and deep learning recognition performance under visual distortions. In *2017 26th international conference on computer communication and networks (ICCCN)*, pages 1–7. IEEE, 2017.
- Peijie Dong, Lujun Li, and Zimian Wei. Diswot: Student architecture search for distillation without training. *IEEE Conference on Computer Vision and Pattern Recognition*, 2023.
- Xuanyi Dong and Yi Yang. Searching for a robust neural architecture in four gpu hours. In *IEEE Conference on Computer Vision and Pattern Recognition*, pages 1761–1770, 2019.
- Thomas Elsken, Jan Hendrik Metzen, and Frank Hutter. Efficient multi-objective neural architecture search via lamarckian evolution. *International Conference on Learning Representations*, 2019.
- Pierre Foret, Ariel Kleiner, Hossein Mobahi, and Behnam Neyshabur. Sharpness-aware minimization for efficiently improving generalization. In *International Conference on Learning Representations*, 2021.
- Ian J Goodfellow, Jonathon Shlens, and Christian Szegedy. Explaining and harnessing adversarial examples. In *International Conference on Learning Representations*, 2015.
- Minghao Guo, Yuzhe Yang, Rui Xu, Ziwei Liu, and Dahua Lin. When nas meets robustness: In search of robust architectures against adversarial attacks. *IEEE Conference on Computer Vision and Pattern Recognition*, 2020.
- Dan Hendrycks and Thomas Dietterich. Benchmarking neural network robustness to common corruptions and perturbations. *International Conference on Learning Representations*, 2019.
- Dan Hendrycks, Norman Mu, Ekin D Cubuk, Barret Zoph, Justin Gilmer, and Balaji Lakshminarayanan. Augmix: A simple data processing method to improve robustness and uncertainty. *International Conference on Learning Representations*, 2020.
- Steffen Jung, Jovita Lukasik, and Margret Keuper. Neural architecture design and robustness: A dataset. In *International Conference on Learning Representations*, 2023.
- Namhoon Lee, Thalaisyasingam Ajanthan, and Philip HS Torr. Snip: Single-shot network pruning based on connection sensitivity. *International Conference on Learning Representations*, 2019.

- Chenxi Liu, Barret Zoph, Maxim Neumann, Jonathon Shlens, Wei Hua, Li-Jia Li, Li Fei-Fei, Alan Yuille, Jonathan Huang, and Kevin Murphy. Progressive neural architecture search. In *European Conference on Computer Vision*, pages 19–34, 2018a.
- Hanxiao Liu, Karen Simonyan, Oriol Vinyals, Chrisantha Fernando, and Koray Kavukcuoglu. Hierarchical representations for efficient architecture search. In *International Conference on Learning Representations*, 2018b.
- Hanxiao Liu, Karen Simonyan, and Yiming Yang. Darts: Differentiable architecture search. *International Conference on Learning Representations*, 2019.
- Liyang Liu, Shilong Zhang, Zhanghui Kuang, Aojun Zhou, Jing-Hao Xue, Xinjiang Wang, Yimin Chen, Wenming Yang, Qingmin Liao, and Wayne Zhang. Group fisher pruning for practical network compression. In *International Conference on Machine Learning*, pages 7021–7032. PMLR, 2021.
- Renqian Luo, Fei Tian, Tao Qin, Enhong Chen, and Tie-Yan Liu. Neural architecture optimization. *Advances in Neural Information Processing Systems*, 31, 2018.
- Aleksander Madry, Aleksandar Makelov, Ludwig Schmidt, Dimitris Tsipras, and Adrian Vladu. Towards deep learning models resistant to adversarial attacks. In *International Conference on Learning Representations*, 2018.
- Joe Mellor, Jack Turner, Amos Storkey, and Elliot J Crowley. Neural architecture search without training. In *International Conference on Machine Learning*, pages 7588–7598. PMLR, 2021.
- Jisoo Mok, Byunggook Na, Hyeokjun Choe, and Sungroh Yoon. Advrush: Searching for adversarially robust neural architectures. In *IEEE Conference on Computer Vision and Pattern Recognition*, pages 12322–12332, 2021.
- Seyed-Mohsen Moosavi-Dezfooli, Alhussein Fawzi, and Pascal Frossard. Deepfool: a simple and accurate method to fool deep neural networks. In *Proceedings of the IEEE conference on computer vision and pattern recognition*, pages 2574–2582, 2016.
- Hieu Pham, Melody Guan, Barret Zoph, Quoc Le, and Jeff Dean. Efficient neural architecture search via parameters sharing. In *International Conference on Machine Learning*, pages 4095–4104. PMLR, 2018.
- Esteban Real, Sherry Moore, Andrew Selle, Saurabh Saxena, Yutaka Leon Suematsu, Jie Tan, Quoc V Le, and Alexey Kurakin. Large-scale evolution of image classifiers. In *International Conference on Machine Learning (ICML)*, 2017.
- Esteban Real, Alok Aggarwal, Yanping Huang, and Quoc V Le. Regularized evolution for image classifier architecture search. In *AAAI Conference on Artificial Intelligence*, 2019.
- Christian Szegedy, Wojciech Zaremba, Ilya Sutskever, Joan Bruna, Dumitru Erhan, Ian Goodfellow, and Rob Fergus. Intriguing properties of neural networks. *International Conference on Learning Representations*, 2014.
- Hidenori Tanaka, Daniel Kunin, Daniel L Yamins, and Surya Ganguli. Pruning neural networks without any data by iteratively conserving synaptic flow. *Advances in Neural Information Processing Systems*, 33:6377–6389, 2020.
- Chaoqi Wang, Guodong Zhang, and Roger Grosse. Picking winning tickets before training by preserving gradient flow. *International Conference on Learning Representations*, 2020.
- Eric Wong, Leslie Rice, and J Zico Kolter. Fast is better than free: Revisiting adversarial training. *arXiv preprint arXiv:2001.03994*, 2020.
- Dongxian Wu, Shu-Tao Xia, and Yisen Wang. Adversarial weight perturbation helps robust generalization. In H. Larochelle, M. Ranzato, R. Hadsell, M.F. Balcan, and H. Lin, editors, *Advances in Neural Information Processing Systems*, 2020.

Yuhui Xu, Lingxi Xie, Xiaopeng Zhang, Xin Chen, Guo-Jun Qi, Qi Tian, and Hongkai Xiong. Pc-darts: Partial channel connections for memory-efficient architecture search. *International Conference on Learning Representations*, 2020.

Hongyang Zhang, Yaodong Yu, Jiantao Jiao, Eric P Xing, Laurent El Ghaoui, and Michael I Jordan. Theoretically principled trade-off between robustness and accuracy. In *International Conference on Machine Learning*, 2019.

Zhao Zhong, Junjie Yan, Wei Wu, Jing Shao, and Cheng-Lin Liu. Practical block-wise neural network architecture generation. In *IEEE Conference on Computer Vision and Pattern Recognition*, pages 2423–2432, 2018.

Barret Zoph and Quoc V Le. Neural architecture search with reinforcement learning. *International Conference on Learning Representations*, 2017.

Barret Zoph, Vijay Vasudevan, Jonathon Shlens, and Quoc V. Le. Learning transferable architectures for scalable image recognition. In *IEEE Conference on Computer Vision and Pattern Recognition*, 2018.

Supplementary Materials

Generalizable Lightweight Proxy for Robust NAS against Diverse Perturbations

A EXPERIMENTAL SETTING

Search space Based on the cell-based neural architecture search space [Zoph et al. \(2018\)](#), we regard the whole network as the composition of repeated cells. Thus, we search for the optimal cell architectures and stack them repeatedly to construct the entire network. In the cell-based search phase, each cell can be represented as a directed acyclic graph (DAG), which has N nodes that represent the feature maps $z_j (j = 1, \dots, N)$ and each edge between arbitrary node i and node j represents an operation $o_{i,j}$ chosen from the operation pool, where $o_{i,j} \in \mathcal{O} = \{o_k, k = 1, 2, \dots, n\}$. Each feature map z_j is obtained from all of its predecessors as follows:

$$x_j = \sum_{i < j} o_{i,j}(x_i) \quad (11)$$

In this work, we utilize NAS-Bench-201 ([Dong and Yang, 2019](#)), and DARTS ([Liu et al., 2019](#)) search space, where different operation pools are used, which are $\mathcal{O} = \{1 \times 1 \text{ conv.}, 3 \times 3 \text{ conv.}, 3 \times 3 \text{ avg. pooling, skip, zero}\}$, and $\mathcal{O} = \{3 \times 3 \text{ conv.}, 3 \times 3 \text{ dil.conv.}, 5 \times 5 \text{ conv.}, 5 \times 5 \text{ dil.conv.}, 7 \times 7 \text{ conv.}, 3 \times 3 \text{ max pooling, } 3 \times 3 \text{ avg. pooling, skip, zero}\}$, respectively. Especially, for the NAS-Bench-201 search space, we additionally use the [Jung et al. \(2023\)](#) dataset that includes robust accuracies of candidate neural architectures in NAS-Bench-201 search space to demonstrate the efficacy of our proposed proxy regarding searching generalized architectures against diverse perturbations and clean inputs.

Adversarial Evaluation To evaluate standard-trained models, we utilize the robust NAS-Bench-201 ([Jung et al., 2023](#)) datasets, allowing us to achieve robust accuracy. On the other hand, to evaluate adversarially-trained models, we construct our own dataset, as described in [Section 4.2](#), enabling us to obtain robust accuracy against adversarial attacks. In all our experiments, we obtain robust accuracy on CIFAR-10 against FGSM attack with an attack size (ϵ) of 8.0/255.0 and attack step size (α) of 8.0/2550.0 while we utilize robust accuracies against FGSM attack with attack size (ϵ) of 4.0/255.0 on ImageNet16-120.

B EXPERIMENTAL RESULTS

B.1 ABLATION ON EACH COMPONENT OF CROZE

In [Section 3.3](#), we introduce our proxy, which consists of three components: feature consistency, parameter similarity, and gradient similarity. We discuss the importance of considering all three components to accurately evaluate the robustness of neural architectures in a random state ([Section 3.1](#)). To analyze the contributions of each factor, we conduct an ablation study in both the NAS-Bench-201 search space and the DARTS search space.

We find that relying solely on feature consistency in a random state is insufficient to evaluate the robustness of architectures. The proxy with only feature consistency shows a lower correlation in both standard training and adversarial training scenarios compared to CRoZe in the NAS-Bench-201 search space ([Table 6a](#) and [Table 6b](#)). This indicates that high scores obtained based on feature consistency on a single batch may not accurately reflect the performance across the entire dataset. On the other hand, when parameter or gradient similarity is added to the proxy, the correlation consistently improved, suggesting that these factors complement feature consistency by imposing stricter constraints on the parameter space and convergence directions, respectively. While the proxy considering only parameter and gradient similarity achieves better Spearman’s ρ compared to our proxy, the top-3 architectures chosen by our proxy exhibit higher average performance than those discovered by the proxy without feature consistency ([Table 7a](#)). Moreover, CRoZe selects the same top-1 candidate architecture as the proxy without feature consistency in the NAS-Bench-201 search space.

Table 6: Comparison of Spearman’s ρ between the actual accuracies and the proxy values on CIFAR-10 in the NAS-Bench-201 search space. Clean stands for clean accuracy and robust accuracies are evaluated against adversarial perturbations (FGSM Goodfellow et al. (2015)) and common corruptions (CC. (Hendrycks and Dietterich, 2019)). Avg. stands for average Spearman’s ρ values with all accuracies.

Proxy components			Standard-Trained				Proxy components			Adversarially-Trained				
Feature	Parameter	Gradient	Clean	FGSM	CC.	Avg.	Feature	Parameter	Gradient	Clean	FGSM	PGD	HRS(FGSM)	HRS(PGD)
✓	–	–	0.718	0.701	0.341	0.587	✓	–	–	0.602	0.295	0.329	0.442	0.404
✓	✓	–	0.750	0.762	0.384	0.632	✓	✓	–	0.677	0.343	0.431	0.542	0.527
✓	–	✓	0.822	0.824	0.434	0.693	✓	–	✓	0.707	0.405	0.489	0.587	0.573
–	✓	✓	0.824	0.827	0.437	0.696	–	✓	✓	0.731	0.422	0.507	0.610	0.595
✓	✓	✓	0.823	0.826	0.436	0.695	✓	✓	✓	0.723	0.417	0.501	0.602	0.588

(a) Standard-Trained

(b) Adversarially-Trained

Table 7: Comparisons of the final performance of the searched network in NAS-Bench-201 and DARTS search space on CIFAR-10. **Bold** and underline stands for the best and second.

Proxy components			Standard-Trained (Top-1)				Standard-Trained (Top-3)				Proxy Components			Standard-Trained				
Feature	Parameter	Gradient	Clean	FGSM	CC.	Avg.	Clean	FGSM	CC.	Avg.	Feature	Parameter	Gradient	Clean	CC.	FGSM	HRS	Avg.
✓	–	–	93.30	44.30	55.62	64.41	92.93	37.60	54.03	61.52	✓	–	–	94.37	72.26	16.87	28.62	53.78
✓	✓	–	93.70	45.80	56.93	65.48	93.63	48.20	55.39	65.74	✓	✓	–	94.99	74.06	16.82	28.58	53.86
✓	–	✓	93.70	45.80	56.93	65.48	93.63	48.20	55.39	65.74	✓	–	✓	94.30	74.91	16.67	28.33	53.55
–	✓	✓	93.70	45.80	56.93	65.48	93.43	41.37	55.30	63.37	–	✓	✓	94.34	74.46	15.71	26.93	52.61
✓	✓	✓	93.70	45.80	56.93	65.48	93.93	43.87	56.11	<u>64.64</u>	✓	✓	✓	<u>94.45</u>	<u>74.63</u>	22.38	33.19	56.41

(a) NAS-Bench-201 search space

(b) DARTS search space

We further conduct ablation experiments on CIFAR-10 in the DARTS search space, which contains about 10^{19} number of candidate architectures that is significantly larger than the NAS-Bench-201 search space containing 15625 architectures. The proxy without feature consistency yielded architectures with poor robust accuracies, while the architectures selected by our proxy consistently outperformed the former on both clean and perturbed images (Table 7b). Furthermore, the average performance of the architectures chosen by the proxy based solely on feature consistency shows even higher than that of the architectures discovered by the proxy without considering feature consistency. This clearly demonstrates the influential role of feature consistency in evaluating robustness. Overall, our proposed proxy effectively searches high-performing architectures by employing consistency across features, parameters, and gradients to estimate the robustness of the given architectures within a single gradient step. The overall algorithm of CRoZe is described in Algorithm 1.

B.2 ABLATION ON PERTURBATION TYPE OF INPUT

In Section 4.4, we demonstrate the independence of our proxy from specific perturbation types applied to the input. This is evident in the consistency of clean and perturbed inputs captured by CRoZe, regardless of the perturbation types, thereby effectively capturing the characteristics of robust architectures. To further evaluate CRoZe, we conduct additional experiments on diverse tasks such as CIFAR-100 and ImageNet16-120 within the NAS-Bench-201 search space. As shown in Table 8, CRoZe exhibits good correlation, and even when random Gaussian noise is utilized instead of adversarial perturbations to generate the perturbed inputs on CIFAR-100, the gap is merely 0.001. This further emphasizes the ability of CRoZe to capture the robustness of the given neural architectures across tasks and perturbations without overfitting to the utilized perturbation type.

B.3 ASSESSMENT OF CROZE PREDICTIVENESS ON ADVERSARIALLY-TRAINED MODELS

As we verify the predictiveness of CRoZe with 300 standard-trained models in the NAS-Bench-201 search space in Section 4.4, we further validate the predictiveness of our proxy against adversarially-trained models. To achieve adversarial robustness, we adversarially-train 300 randomly sampled architectures from NAS-Bench-201 search space on the entire CIFAR-10 dataset, following (Wong et al., 2020). We then compute Spearman’s ρ between the values obtained from the fully-adversarially-trained states and single-step trained states associated with our proxy and each consistency component.

Surprisingly, our proxy demonstrates a strong correlation of 0.983 between the proxy value obtained from a fully-trained state and a single-step trained state (Figure 7). This indicates that our proxy accurately predicts the robustness of architectures even when they are adversarially-trained. Furthermore, each individual component of the proxy also exhibits a high correlation, suggesting that a strong

Algorithm 1: Consistency-based Robust Zero-cost Proxy (CRoZe).

Input: A single batch of given dataset $B = \{(x, y)\}$, network $f_\theta(\cdot)$ consists of M layer, which is architecture \mathcal{A} with parameterized by θ

Output: Proxy value, $CRoZe$

```

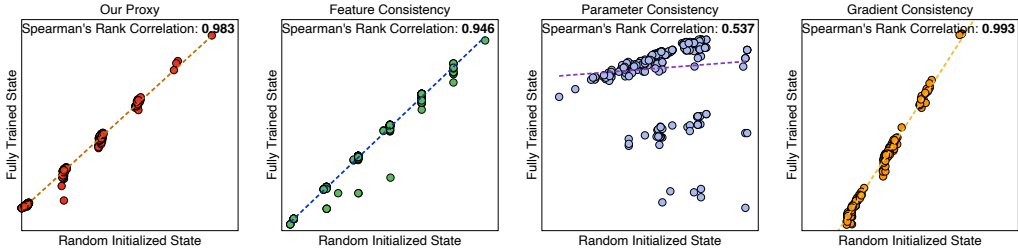
/* Estimate robust network  $f_{\theta^r}$  as done in Eq. 3. */
for  $m = 1, \dots, M$  do
     $\theta_m^r \leftarrow \theta_m + \beta * \frac{\nabla_{\theta_m} \mathcal{L}(f_\theta(x), y)}{\|\nabla_{\theta_m} \mathcal{L}(f_\theta(x), y)\|} * \|\theta_m\|$ 
/* Generate perturbed input  $x'$  using  $f_{\theta^r}$ . as done in Eq. 4 */
 $\delta = \epsilon \text{sign}(\nabla_x \mathcal{L}(f_{\theta^r}(x), y))$ 
 $x' = x + \delta$ 
/* Calculate consistency in features, parameters, and gradients
as done in Section 3.3 */
/* Calculate gradients of both clean network  $f_\theta$  and robust
network  $f_{\theta^r}$  */
 $g = \nabla_\theta \mathcal{L}(f_\theta(x), y)$ 
 $g^r = \nabla_{\theta^r} \mathcal{L}(f_{\theta^r}(x'), y)$ 
/* Single gradient step for clean network  $f_\theta$  and robust network
 $f_{\theta^r}$  */
 $\theta_1 \leftarrow \theta - \gamma g$ 
 $\theta_1^r \leftarrow \theta^r - \gamma g^r$ 
for  $m = 1, \dots, M$  do
    /* Feature consistency */
     $\mathcal{Z}_m(f_\theta(x), f_{\theta^r}(x')) = 1 + \frac{z_m \cdot z_m^r}{\|z_m\| \|z_m^r\|}$ 
    /* Parameter consistency */
     $\mathcal{P}_m(\theta_1, \theta_1^r) = 1 + \frac{\theta_{1,m} \cdot \theta_{1,m}^r}{\|\theta_{1,m}\| \|\theta_{1,m}^r\|}$ 
    /* Gradient consistency */
     $\mathcal{G}_m(g, g^r) = \left| \frac{g_m \cdot g_m^r}{\|g_m\| \|g_m^r\|} \right|$ 
 $CRoZe = \sum_{m=1}^M \mathcal{Z}_m \times \mathcal{P}_m \times \mathcal{G}_m$ 
return  $CRoZe$ ;

```


Table 8: Comparison of Spearman’s ρ between the actual accuracies and the proxy values on CIFAR-100 and ImageNet16-120 in NAS-Bench-201 search space. Avg. stands for average Spearman’s ρ values with all accuracies within each task.

Perturbation Type	CIFAR-100							ImageNet16-120		
	Clean	FGSM	Weather	Noise	Blur	Digital	Avg.	Clean	FGSM	Avg.
Gaussian Noise	0.774	0.693	0.744	0.261	0.454	0.678	0.601	0.741	0.671	0.706
Adversarial	0.787	0.693	0.747	0.251	0.450	0.682	0.602	0.769	0.696	0.733

Figure 7: Spearman’s ρ in our proxy and each consistency component between the neural architectures with single-step trained states and fully-trained states against clean and perturbed images. All models are trained only on adversarially-perturbed images.



predictiveness of our proxy against diverse perturbations does not rely on a dominant component, but rather on the overall precise evaluation provided by the combination of components.

B.4 END-TO-END PERFORMANCE ON IMAGENET16-120

Table 9: Comparisons of the final performance and required computational resources of the searched network in DARTS search space on ImageNet16-120.

NAS Method	NAS Training-free	Params (M)	# GPU	Batch Size	Standard-Trained			
					Clean	CC.	FGSM	HRS
PC-DARTS (Xu et al., 2020)		5.30	8	1024	50.58	14.36	0.15	0.30
DrNAS (Chen et al., 2020)		5.70	8	512	49.63	13.42	0.21	0.42
AdvRush (Mok et al., 2021)		4.20	1	64	38.72	10.39	0.11	0.22
GradNorm (Abdelfattah et al., 2021)	✓	5.90	1	8	39.13	10.75	0.23	0.46
SynFlow (Abdelfattah et al., 2021)	✓	6.13	1	8	43.73	12.10	0.15	0.30
CRoZe	✓	5.87	1	8	47.90	13.35	0.32	0.64

We further validate the final performance of the searched neural architectures by CRoZe and compare the required computational resources with existing NAS frameworks including robust NAS (AdvRush (Mok et al., 2021)), clean one-shot NAS (PC-DARTS (Xu et al., 2020), DrNAS (Chen et al., 2020)) and clean zero-shot NAS (SynFlow and GradNorm (Abdelfattah et al., 2021)), on ImageNet16-120 in the DARTS search space. Similar to Section 4.3, we sample the same number (5,000) of candidate architectures using the warmup+move strategy for both clean-zero shot NAS and CRoZe.

The NAS Training-free methods such as GradNorm, SynFlow, and CRoZe only require a single GPU with a batch size of 8 to search for the architectures on the ImageNet16-120 dataset. In contrast, the existing clean one-shot NAS methods require 8 GPUs with much larger batch sizes. Moreover, NAS-Training-free methods consume less than 3000MB of memory, while both clean one-shot NAS and robust NAS need at least 3090 RTX GPU, which is available at 24000MB of memory. With its superior computational efficiency, CRoZe enables rapid neural architecture search and achieves the best HRS accuracy while maintaining comparable clean and common corruption accuracies. all at a much lower computational cost (Table 9). These demonstrate the effectiveness of CRoZe for rapid and lightweight robust NAS across diverse tasks (i.e., CIFAR-10, CIFAR-100, and ImageNet16-120) and perturbations (i.e., adversarial perturbations and common corruptions).